PRIORITIZING WAVE PASSAGE AND SOIL-STRUCTURE INTERACTION EFFECTS FOR THE SEISMIC FRAGILITY OF MULTI-SPAN BRIDGES

S.S.F. Mehanny[(1)], O.M.O. Ramadan[(2)], A.A-M. Kotb[(3)]

[(1)] *Professor, Structural Engineering Department, Cairo University, Egypt, and DAR Al-Handasah Bridge Department, Egypt, E-mail: sameh.mehanny@stanfordalumni.org*

[(2)] *Professor, Structural Engineering Department, Cairo University, Egypt. Presently, Dean of Higher Technological Institute (HTI) 10th of Ramadan city, Egypt; E-mail: omoramadan@yahoo.ca*

[(3)] *Lecturer, Higher Institute of Engineering at El-Shorouk City, Cairo, Egypt; E-mail: aminkotb@hotmail.com*

Abstract

Uniform ground motion excitation is typically assumed in seismic response analysis of structures with somehow limited footprints. In essence, seismic design of bridges is customarily performed assuming identical signal at all bridge supports. However, in fact, ground motions do vary at different supports especially for extended structures such as long bridges, dams, and pipelines. On another issue, bridges, which are often supported on deep foundations, are commonly analyzed using fixed base assumption. Obviously, such analysis does not account for the pile-soil interaction effects on the bridge seismic response. This is primarily due to the wide consensus among practitioners that fixed base entails a more conservative design. Nevertheless, many researchers revealed that ignoring soil-structure interaction, SSI, is behind several unsafe cases in practice. Hence, this paper focuses on assessing the effects of non-synchronized motion (due to the difference in the ground motion arrival time at different bridge supports) on the seismic performance of long multi-span box girder bridges supported on deep foundation; the severity of such effects when simultaneously considering soil-structure interaction is also addressed. The study is carried out on a nine-span continuous bridge with a total length of 430m resting on a piled foundation system embedded in sand soils. Three different sand soil profiles are investigated representing cases of medium to stiff soil. Nonlinear incremental dynamic analyses under eighteen real bedrock earthquakes are conducted in the longitudinal direction of the bridge for different apparent wave propagation velocities (namely, 100, 420, 1000 m/s, and ∞ designating synchronized signals at all supports). Results are hence manipulated through a probabilistic analysis framework to generate fragility curves associated with various performance levels (viz., Operational, Life Safety, and Complete Collapse) and considering modeling and capacity uncertainties. The Peak Ground Velocity, PGV, is tested and adopted herein to serve as an optimal intensity measure, IM, since it is well appreciated in the specialized literature that velocity-related IMs per se are endorsed for fragility analysis of bridges considering SSI. The fragility curves are finally put into perspective to examine the mutual effect (and severity) of non-synchronized support motions and SSI on the seismic performance and vulnerability of investigated long multi-span bridges.

Among the key findings it has been demonstrated that to avoid overestimating safety at various performance levels, modeling SSI is recommended as it leads to a lower PGV resistance of the bridge. In addition, concurrently modeling wave passage effects is equally important for a conservative seismic vulnerability assessment. It is however worth noting that PGV may lose some of its optimality as a good candidate IM as the wave passage effects become more pronounced and as the soil becomes remarkably less stiff. A final note is that if the dominant apparent wave velocity is not precisely identified beforehand, it is recommended to investigate several appropriate values especially when targeting lower performance levels (namely, operational and life safety limit states), while for the collapse limit state, the lowest possible apparent wave velocity is likely to entail the most critical scenario for estimating bridge fragility.

Keywords: *multi-span bridges; wave passage; soil-structure interaction; fragility curves; performance levels*

1. Introduction

Uniform ground motion excitations and fixed supports are often considered as a typical assumption in practice for analysis and design of bridges. Although many bridges are typically supported on deep foundation systems, SSI is commonly ignored due to a general belief among experts that ignoring it results in a more conservative design. However, it has been reported that disregarding SSI is behind several unsafe cases in practice [1]. On the other hand, uniform ground motions are also typically assumed in seismic analysis of bridges despite the fact that in extended structures, such as continuous multiple-span bridges, earthquake motions do vary from support to support – a phenomenon known as Spatially Variable Seismic Ground Motions, SVSM [2].

The current paper addresses the mutual effect of SSI and SVSM resulting from wave passage effects on the seismic performance of continuous box-girder bridges through generating fragility curves. The effect of SVSM has been always considered in the present research whether SSI is modeled or ignored. In addition, the effect of uncertainties in both modeling and capacity are considered in the prediction of bridge vulnerability.

2. Spatially Variable Seismic Ground Motions, SVSM

Earthquake motions travel from earthquake focus to structure supports in different paths resulting in different ground motion excitations at each support [3]. SVSM is caused by [4,5]: loss of coherency due to earthquake wave reflections and refractions; variation of local soil; loss in motion attenuation resulting from energy dissipation with wave spreading; and, wave passage effects due to variation of the arrival time of the seismic waves between structure supports as seismic waves travel with finite apparent velocity. The wave passage effect consequently causes the structure to experience varying ground motion excitations leading to out-of-phase displacements. These out of phase motions affect the seismic response of the bridge showing some dynamic effects (generated due to inertia forces resulting from earthquake acceleration) and some pseudo-static effects (resulting from the out-of-phase displacement). The latter vanishes in case of uniform excitation [6,7]. The severity of the wave passage effect on the structure's response depends on the earthquake frequency content and on the difference in the wave arrival time [8].

3. Fragility Analysis

Fragility curves provide a graphical representation for the probability of reaching or exceeding a certain predefined performance limit state (representing the amount of damage expected in structure) at a given earthquake intensity [9]. An analytical fragility function is adopted throughout this study to determine bridge performance at different earthquake intensities by the mean of incremental dynamic analysis (IDA) as per [10]. The accuracy of fragility analysis depends on the chosen intensity measure (IM) and its correlation with the measured damage index (DI). The IM is typically chosen depending on the characteristics of both the studied structure and the ground motion excitation [11]. Peak Ground Velocity, PGV, is selected in the present research being one of the highly recommended IMs in SSI problems/applications [12,13]. It is also worth mentioning that several measures adopted in the literature to verify the optimality of a candidate IM [13,14] (namely, Efficiency, Practicality, and Proficiency) have been applied herein to verify the accuracy of selecting the PGV.

Fragility analysis is conducted following procedures adopted in [3,15,16]. Eq. (1) shows the power-law used to generate the deck/pier drift for the various performance limit states considered herein (namely, Operational, Life-safety, and Collapse limit states). The uncertainties associated with the case-study problem is divided into three types. First, the demand uncertainty (β_D) resulting from the difference between analysis response and the expected value calculated from Eq. (1). Second, modeling uncertainty (β_M) due to inaccuracies in the analysis model. Finally, the capacity uncertainty (β_C) emerging from inaccuracies in the pre-set performance limit states. The total uncertainties (β) is calculated by Eq. (2).

$$S_D = \alpha \times (IM)^b \tag{1}$$

S_D is the median maximum bridge response (pier drift ratio in the current research), IM is the earthquake intensity measure considered herein as the PGV, α and b are regression parameters.

$$\beta = \sqrt{\beta_D{}^2 + \beta_C{}^2 + \beta_M{}^2} \tag{2}$$

Modeling and capacity uncertainties are simply accounted for in the present study through three different distinct and likely occurring values (namely, $\beta_M = \beta_C = 0.1$, 0.2, and 0.3) as per [3,4].

Finally, in a fragility analysis context, the probability of exceeding a predefined performance limit state (LS) given the IM of interest (herein PGV) is calculated as follows:

$$P(LS|PGV) = 1 - \phi\left[\frac{\lambda_{CL} - \lambda_{D|PGV}}{\sqrt{\beta_D{}^2 + \beta_C{}^2 + \beta_M{}^2}}\right] \tag{3}$$

Where ϕ is the standard normal distribution function, λ_{CL} is the ln(median pier drift capacity for a particular performance limit state), $\lambda_{D|PGV}$ is ln(calculated median demand pier drift given PGV from the best fit assumed power-law relationship).

4. Case study

A continuous multi-span bridge consisting of nine spans (40+7×50+40m) with a total length of 430m as shown in Fig. 1 is adapted from [3] with the introduction of the piled foundation system. The bridge system is designed to resist a moderate earthquake with an effective PGA of 0.25g [17] and considering a response modification factor of 5 relying on inherent design ductility as per [18]. The bridge deck is post-tensioned with double vents as shown in *Fig. 2*-a and is supported on 8 piers (10 meters high each with a cross-section as shown in *Fig. 2*-b) and two abutments. The bridge deck is monolithically connected to the two central piers thus preventing both relative translation and rotation between the deck and the top of piers, while one adjacent pier at each side of the two central monolithic piers are connected to the bridge deck through fixed bearings allowing only for rotation while preventing relative translation between pier and deck. The four remaining outer piers and the two abutments feature guided bearings that allow for rotation as well as longitudinal movement of the deck relative to the pier due to thermal effects of the bridge deck. The deck-abutment connection is also designed with a large gap in order to prevent pounding between deck and abutment due to earthquake excitations.

The bridge piers are supported on pile-caps (12×9×2 m) resting on twelve 1 m-diameter piles penetrating sandy soils as shown in Fig. 3. The bridge piles are 25m long penetrating a sand layer with a total thickness of 52m above the bed-rock level as shown in Fig. 5. Three types of sandy soils are considered: (1) very dense, (2) dense, and (3) compacted sand. The selected soil types feature shear velocities equal to 420, 360, and 240 m/s for Soils 1, 2, and 3, respectively (refer to [19,20] for more details regarding the considered soil properties).

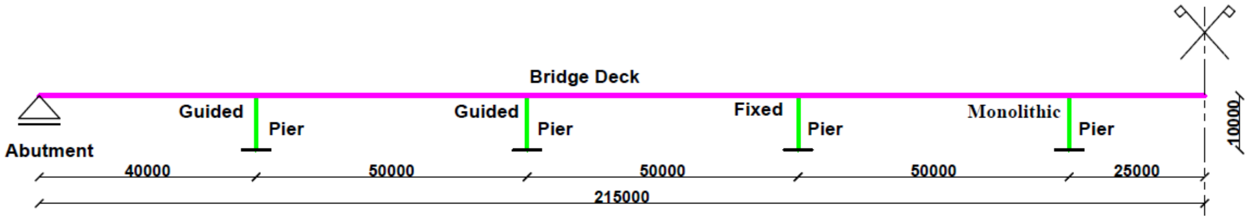

Fig. 1 – Schematic elevation for the case-study bridge with rigid foundations [3], Dimensions are in mm

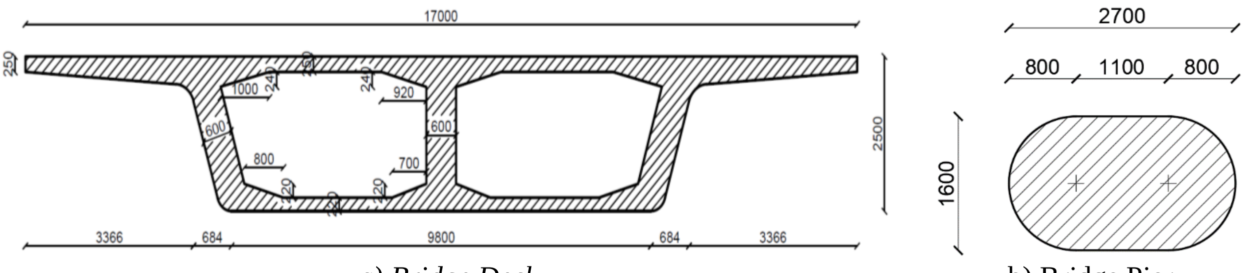

a) Bridge Deck b) Bridge Pier

Fig. 2 – Bridge typical cross-sections, Dimensions are in mm [3]

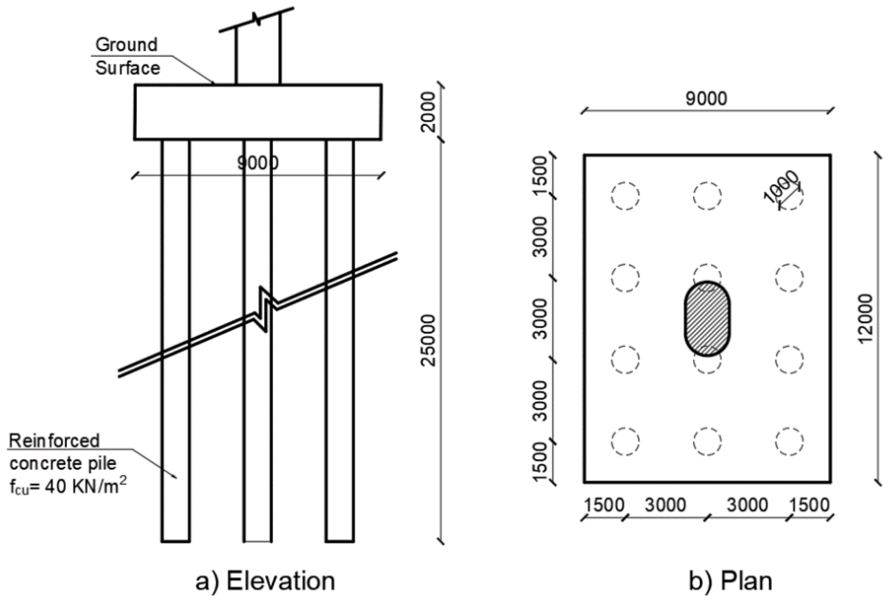

Fig. 3 – Typical bridge foundation system, Dimensions are in mm

5. Numerical Models

Two types of finite element models are developed using OpenSees [21]. The first model considers the bridge with a fixed base assumption (i.e. ignoring SSI effect), while the second model contains the pile-soil system enabling the effect of SSI to be considered. The bridge is analyzed considering the inelastic behavior in both the bridge piers and the soil, while both the pile-foundation (namely piles and pile cap) and the bridge deck are designed to remain elastic during the earthquake, and hence inelastic behavior is not expected [22]. In addition, the geometric nonlinearity due to the P-Δ effect is considered.

5.1 The Fixed base Model

This model considers only the bridge with its foundation system assumed to be fixed (ignoring SSI effect). A two-dimensional model was developed for the longitudinal direction of the bridge system. The bridge deck is modeled using an equivalent elastic frame element, while bridge piers are modeled by an equivalent beam-column elements with concentrated plastic hinges at the ends as per Ibarra lumped plastic model [23,24].

5.2 Soil-Foundation-Bridge Model, SFB

The second model resembles the first model while replacing the fixed base by the pile-soil system as shown in Fig. 4 and Fig. 5. The SFB model is developed following guidelines in [25–29]. The pile-soil system consists of two main parts. The first part is the soil medium consisting of soil columns modeled using nonlinear Pressure Depend Multi-Yield Material (PDMY) developed in OpenSees by [30] based on the Drucker–Prager yield model capable of representing the inelastic response of cohesionless soil. The soil columns are connected to the piles through nonlinear complex interfacing elements. The soil columns are modeled using plane strain elements with a thickness large enough to enforce the free-field motion. The interfacing elements capture the nonlinear interaction between the pile and the surrounding soil in addition to the soil radiational damping (refer to [19] for more details). The second part of the foundation system is the concrete pile-cap that is represented using linear plane strain elements that rest on 12 piles modeled using equivalent elastic frame elements (since inelastic behavior is not expected). The adopted modeling technique provides an acceptable accuracy along with some computational efficiency that is sought to run the overwhelming number of analyses required for vulnerability analysis.

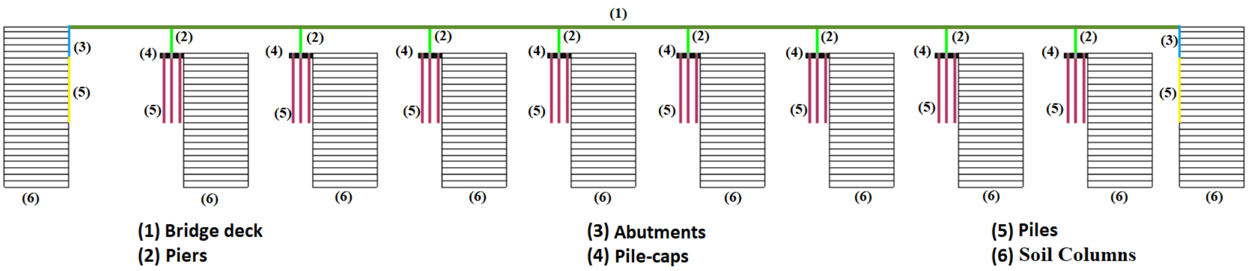

Fig. 4 – The Soil-Foundation-Bridge Model Used in Analysis (For clarity a coarse mesh is shown for the soil column)

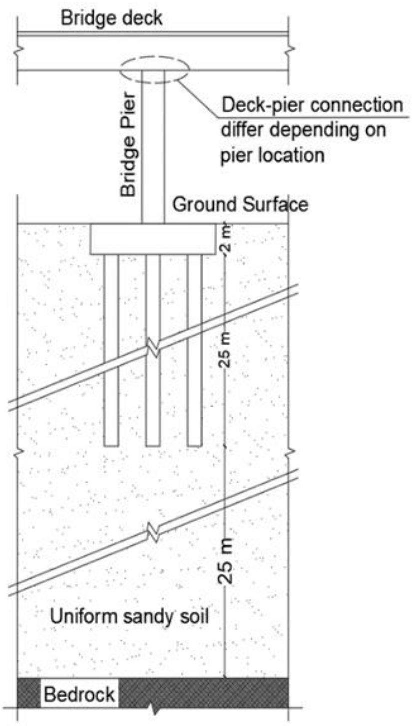

a) Typical details at pier location

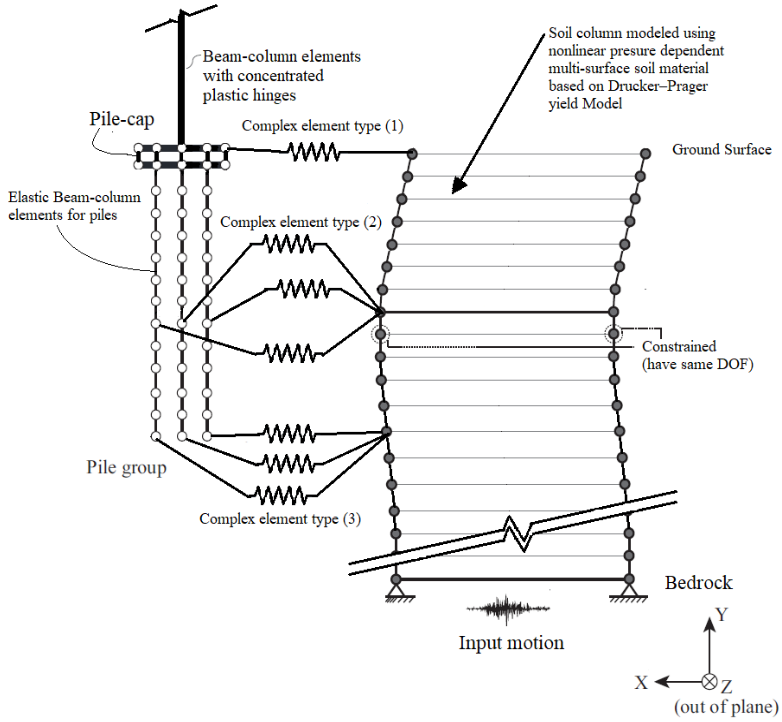

b) Schematic of the typical finite element model of the soil-pile system

Fig. 5 – Schematic of typical soil-pile system

6. Earthquake Records

In order to generate required fragility curves, an ensemble of eighteen real earthquake records are gathered from [31]. All records are selected for rock soils to be suitable for application at the bedrock level to eliminate uncertainties related to the difference in soil type and avoid the need for a deconvolution process [13]. As for the fixed base model, a free-field analysis is conducted using soil columns having the same soil characteristics as the ones in the SFB model to provide earthquake excitations at the bridge fixed support level.

7. Analysis Methodology

Incremental dynamic analysis (IDA) is conducted in the bridge longitudinal direction for the preselected earthquake records through performing nonlinear time history analysis gradually increasing the earthquake intensity (namely, PGV at bedrock level) to capture the bridge response from the elastic state up to collapse.

The analysis is carried out through three stages in order to capture the soil conditions before and after construction:

First stage: only the soil columns are modeled and analyzed under own weight to develop initial soil stress before construction.

Second stage: the bridge elements are added, and transient analysis is conducted with high numerical damping to eliminate the vibrations resulting from bridge loads.

Third (i.e., final) stage: the nonlinear time history analysis is conducted on the complete model.

8. Fragility analysis

Fragility curves have been generated for the case-study bridge in the longitudinal direction including the effect of uncertainties for the three preselected performance levels (namely, Operational, Life-Safety, and Collapse limit states). The threshold values for the selected performance states are considered according to the SEAOC Seismic design manual [32] as shown in Table 1. It is also worth noting that the collapse threshold value has been calculated through nonlinear pushover analysis and found to be 2.56% on average, agreeing with SEAOC recommended values.

Table 1 – Threshold values for bridge drift in the longitudinal direction [32]

Performance limit	**Damage Description**	**Deck Drift (%)**
Fully Operational	Negligible	<0.2
Operational (LS-1)	Minor damage in structure elements (i.e. local yielding, local buckling), without visible fractures.	0.2-0.5
Life safety (LS-2)	Observed damages in structure elements (i.e. Plastic hinge, buckling, isolated connection), with visible fractures.	0.5-1.5
Complete Collapse (LS-3)	-----	>2.5

Fragility curves for the pre-selected performance levels – with and without SSI – are shown in Fig. 6 for three studied apparent velocities (namely, 100, 420, and 1000 m/s) in addition to the uniform excitation, assuming $\beta_M = \beta_C = 0.1$ (namely, uncertainties in modeling and capacity).

For the operational limit state, the lowest probability of exceedance is found to be at the lowest studied apparent velocity (namely, 100 m/s) contrary to the case of larger performance limit states, especially in the case where SSI is considered. Besides, for higher velocities (1000 m/s and infinity), SSI tends to impose a larger probability of exceedance compared to the fixed base case (i.e., SSI ignored) especially for Soil 1 and Soil 3.

For the life-safety limit state, the highest probability of exceedance for low to medium earthquake intensities is found at the lowest studied apparent velocity (namely, 100 m/s), while the apparent velocity of 420 m/s scores the highest probability of exceedance at high intensity seismic excitations (i.e., at larger PGV). Also, similar to the behavior found in the operational limit state, SSI shows a higher probability of exceedance compared to the fixed base assumption (i.e., disregarding SSI) especially at highest investigated apparent velocities (1000 m/s and infinity).

Finally, for the collapse limit state, the collapse probability increases with the reduction in the apparent velocity for all considered soil types, except at high earthquake intensities (viz. bedrock PGV above 1.4 m/s) featuring a collapse probability of exceedance of about 85% and larger. The uniform earthquake excitation even shows the highest collapse probability. Moreover, considering SSI tends to increase the probability of collapse for all investigated soils especially at large apparent velocities such as 1000 m/s and the uniform excitation.

In general, SSI shows an increase in the probability of exceedance for all studied performance/damage limit states compared to the fixed base case, especially at high apparent velocities. In addition, the wave passage effect increases the probability of collapse of the bridge, especially under low apparent velocities, while for other lower performance limit states considered herein, the wave passage effect is highly affected by the level of the limit state, the apparent velocity, the earthquake intensity (i.e., PGV), and the soil type.

As for higher investigated modeling and capacity uncertainties (namely, 0.2 and 0.3), similar behavior is observed (refer to [19]) but not shown herein due to space limitations.

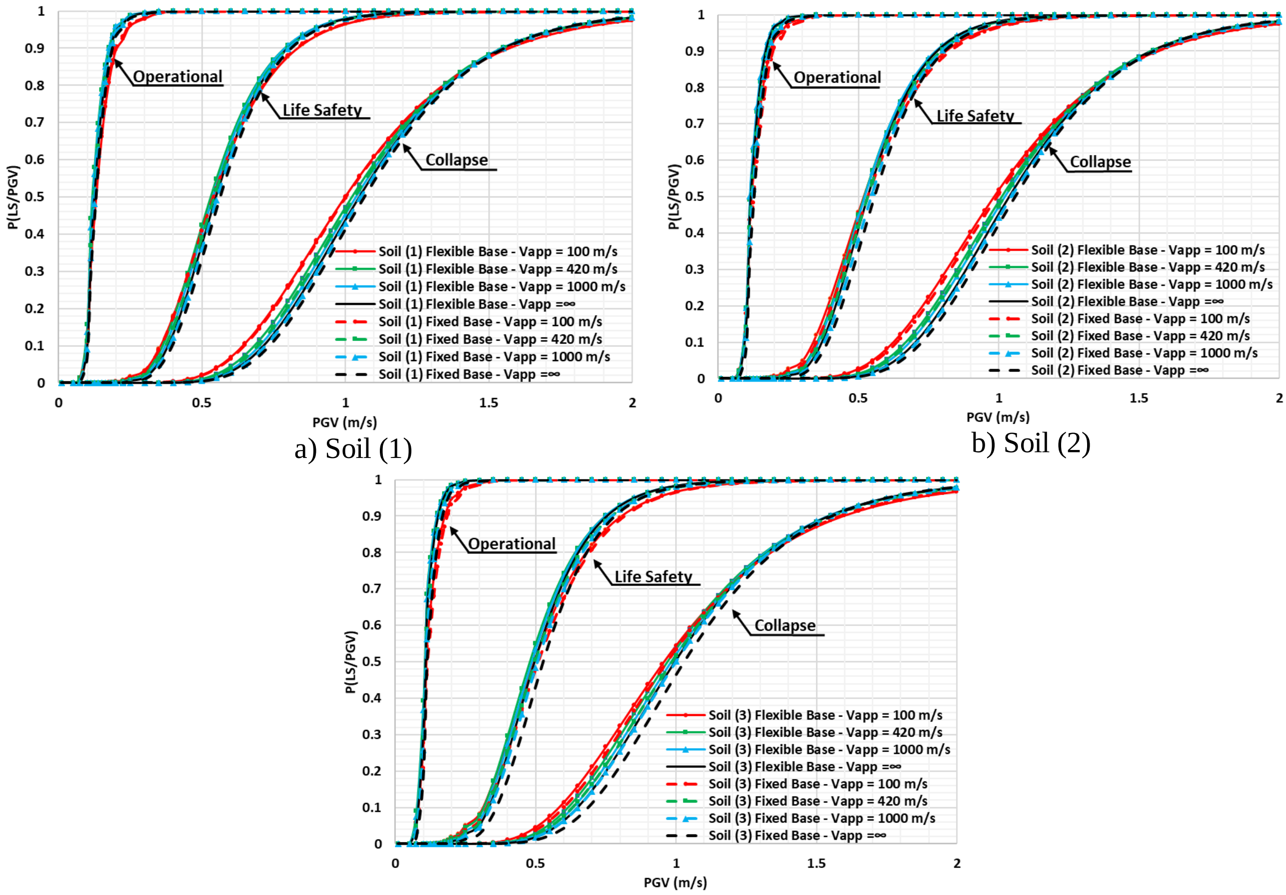

Fig. 6 – Fragility curves of exceeding investigated limit states versus PGV for the preselected apparent velocities (namely, 100, 420, 1000, and infinity) for considered soil types with/without SSI effects assuming capacity and modeling uncertainties with a value of 0.1.

To quantify the mutual effect of SSI and wave passage on the bridge performance, the PGV value causing a probability of exceedance equal to 50% has been selected and compared for all studied cases. This specific value of the probability of exceedance has been chosen since it represents the middle (i.e., pivoting) value of the fragility curve and hence it is not affected by the other modeling and capacity uncertainties inherited in the system. Consequently, comparative results will be directly related to the wave passage and/or SSI effects.

Fig. 7 shows the percentage of change in the PGV corresponding to the probability of exceedance of 50% for the preselected limit states for the investigated apparent velocities compared to the case of uniform excitation. For the operational limit state, the lowest studied apparent velocity (namely 100m/s) shows that the probability of exceedance of 50% takes place at higher PGV (compared to the uniform excitation situation) in all cases where SSI is considered with an increase in value reaching up to 7% for Soil 3. Moreover, as shown in Fig. 7-a, higher apparent velocities lead to this particular probability of exceedance for lower earthquake intensity values (i.e., lower PGV) depending on the soil type and the specific value of the apparent velocity. Finally, the apparent velocity of 420 m/s has the largest impact on the bridge operational limit state compared to other investigated apparent velocities in almost all investigated cases with a reduction in the required PGV reaching up to 8%.

On the other hand, for the life-safety limit state, all cases show a decrease in PGV required to achieve the selected probability of exceedance of 50% compared to the uniform excitation scenario with a reduction reaching up to 5.5%. This effect is more pronounced in the fixed base models (i.e., SSI ignored) compared to the case of flexible base models (i.e., SSI considered). Investigating Fig. 7-b, it could be clearly stated that SSI clearly impacts the effect of wave passage depending on soil type.

, for the collapse limit state, all studied cases (with various apparent velocities) score a reduction in the required PGV compared to the uniform excitation scenario. In other words, the results show that the probability of exceedance of 50% occurs at lower PGV for all studied cases compared to the uniform excitation as shown in Fig. 7-c. Moreover, the lowest investigated apparent velocity (100 m/s) features the highest decrease in required PGV reaching up to 6%. This effect is less pronounced with the increase of the apparent velocity.

Generally speaking, ignoring SSI effects makes the bridge more sensitive to changes in seismic wave apparent velocity (viz. wave passage effects) compared to the cases where SSI is considered. Nonetheless, this does not mean that the fixed base modeling is more critical (and accordingly more conservative) than the flexible base modeling, but it just infers that the wave passage effect is more pronounced in the fixed base case under the same supporting conditions.

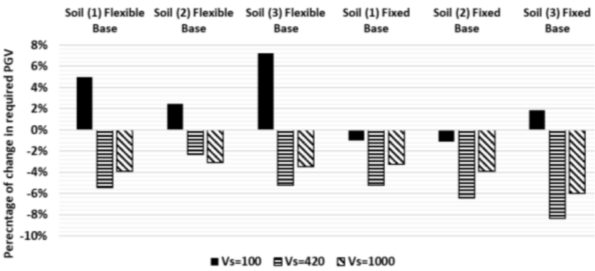

a) Operational limit state

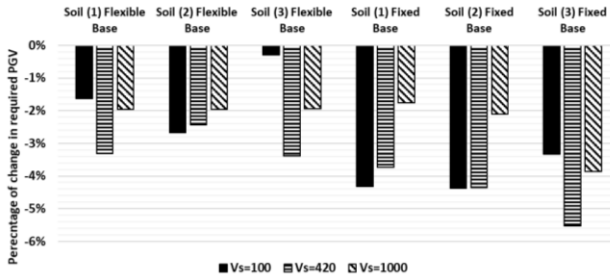

b) Life safety limit state

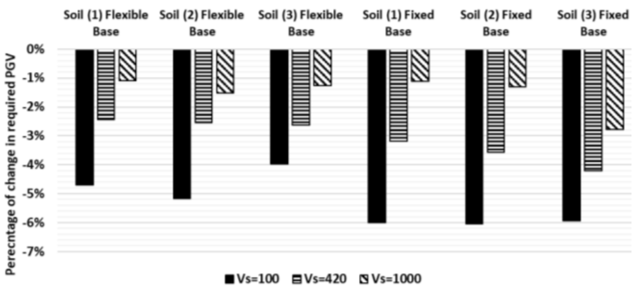

c) Collapse limit state

Fig. 7 – Change in earthquake IM (PGV) required to achieve a probability of 50% for exceeding investigated performance/damage limit states due to the wave passage effects compared to the uniform excitation scenario

Fig. 8 illustrates the effect of SSI on the performance of the bridge in terms of the change in PGV required to achieve a probability of exceedance of 50% under different investigated apparent velocities. Almost all investigated cases reach this pre-selected probability of exceedance at lower PGV values except for

Soil 1 with an apparent velocity of 100 m/s for the operational limit state. The SSI scores the highest impact for the lowest investigated damage limit state (namely, operational limit state) with a reduction in the required PGV reaching up to 5.6%, 9.6%, and 11.4% for Soils 1, 2, and 3, respectively. The impact of SSI drastically decreases for higher performance/damage limit states with a reduction in the PGV capacity reaching only 6% and 3.3% for life-safety and collapse limit states, respectively. In addition, it is found that SSI shows a higher impact on the performance of the bridge for larger apparent velocities compared to lower ones, as it is clear from Fig. 8 that the uniform excitation scenario (with an apparent velocity equal to infinity) features the highest reduction in the PGV corresponding to 50% probability of exceedance for almost all investigated cases followed by the apparent velocity of 1000 m/s. Finally, it could be also generally stated that weak soil (namely, Soil 3) has the highest effect for SSI for all investigated cases.

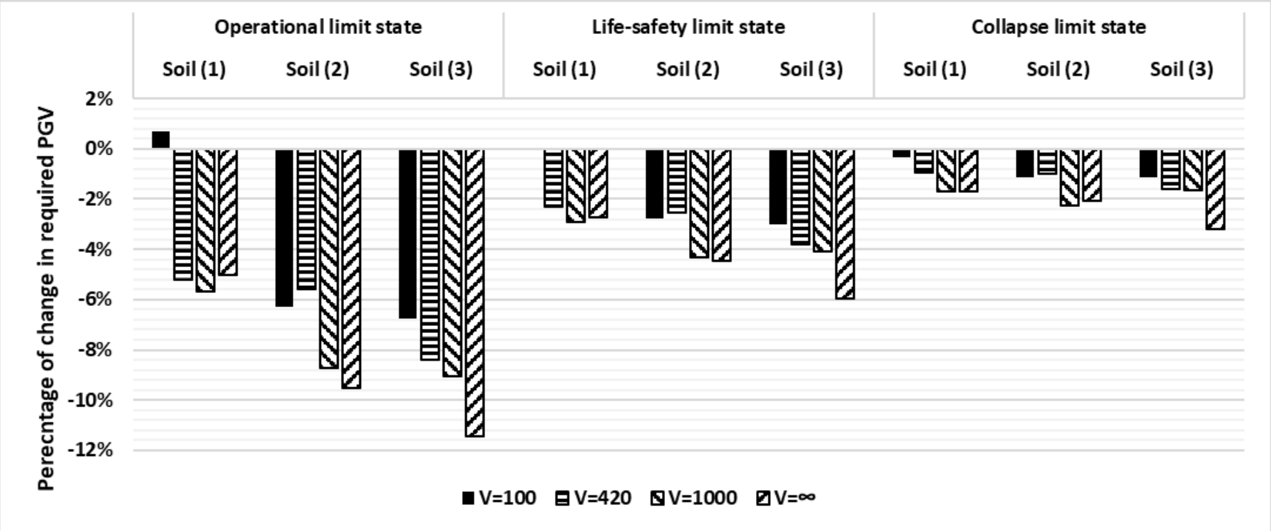

Fig. 8 – Change in earthquake IM (PGV) required to achieve a probability of 50% for exceeding investigated performance/damage limit states due to SSI effects compared to the fixed base modeling.

9. Concluding Remarks

This paper investigates both SSI and wave passage effects on the seismic performance of long continuous multiple-span bridges supported on piled foundation penetrating sandy soil through performing fragility analysis. Three types of sandy soil are investigated (namely, very dense, dense, and compacted sand) for three apparent velocities (namely, 100, 420, 1000 m/s) in addition to the uniform excitation scenario (with an apparent velocity equals to infinity). Analysis of results revealed the following main conclusions:

- The probability of exceeding investigated performance/damage limit states is generally higher in the cases where the wave passage effect is considered compared to the uniform excitation scenario.
- Soil structure interaction increases bridge probability of exceeding various investigated performance limit states compared to the fixed base modeling under the same conditions.
- Operational and life-safety limit states are more affected by the wave passage effects without a clear general trend as the behavior is sensitive to apparent wave propagation velocity, earthquake intensity (viz. PGV herein), and soil type/stiffness. Nevertheless, the probability of collapse of the bridge increases as the apparent velocity decreases.
- Wave passage effect is more pronounced for fixed base models than for flexible base ones. However, considering SSI results in a higher total probability of exceedance compared to fixed base assumption.
- The effects of SSI and wave passage on the probability of exceedance of investigated performance limit states somehow decrease with the increase in the earthquake intensity in terms of PGV.

- Compared to the uniform excitation scenario, wave passage reduces the mean PGV required to achieve various investigated performance/damage limit states by up to 6%.
- Considering SSI reduces the mean PGV resistance of the bridge compared to the fixed base modeling; this reduction in the PGV reaches up to 11.4% for operational limit state while it decreases at higher damage limit states reaching values of 5.6% and 3.1% for life-safety and collapse limit states, respectively.

Finally, it is concluded that SSI and wave passage effects should be simultaneously considered to avoid underestimation of the probability of exceedance of performance/damage limit states. Moreover, apparent wave velocity should be accurately addressed as its effect varies from one soil type to another depending on its particular value, especially for lower damage limit states such as the operational and life-safety performance levels.

10. Copyrights

11. References

[1] Ucak A, Tsopelas P. Effect of Soil–Structure Interaction on Seismic Isolated Bridges. J Struct Eng 2008;134:1154–64. doi:10.1061/(ASCE)0733-9445(2008)134:7(1154).

[2] Xiong M, Huang Y, Zhao Q. Effect of travelling waves on stochastic seismic response and dynamic reliability of a long-span bridge on soft soil. Bull Earthq Eng 2018;16:3721–38. doi:10.1007/s10518-018-0316-x.

[3] Mehanny SSF, Ramadan OMO, El Howary HA. Assessment of bridge vulnerability due to seismic excitations considering wave passage effects. Eng Struct 2014;70:197–207. doi:10.1016/j.engstruct.2014.04.010.

[4] Ramadan OMO, Mehanny SSF, Elhowary HA. Seismic vulnerability of box girder continuous bridges under spatially variable ground motions. Bull Earthq Eng 2015;13:1727–48. doi:10.1007/s10518-014-9683-0.

[5] Zerva A. Spatial Variation of Seismic Ground Motions: Modeling and Engineering Applications. 1st ed. CRC Press Taylor & Francis Group; 2009.

[6] Alam MI, Kim D. Spatially Varying Ground Motion Effects on Seismic Response of Adjacent Structures considering Soil-Structure Interaction. Adv Struct Eng 2014;17:131–42. doi:10.1260/1369-4332.17.1.131.

[7] Wang D, Li Y, Hao S, Zhao D. Wave-Passage Effect of Earthquake Loadings on Long Structures. Int J Struct Stab Dyn 2016;16:1550037. doi:10.1142/S0219455415500376.

[8] Zhao Y, Li Y, Zhang Y, Kennedy D. Nonstationary seismic response analysis of long-span structures by frequency domain method considering wave passage effect. Soil Dyn Earthq Eng 2018;109:1–9. doi:10.1016/j.soildyn.2018.02.029.

[9] Porter K. A Beginner ' s Guide to Fragility , Vulnerability , and Risk. Colorado: University of Colorado Boulder; 2019.

[10] Vamvatsikos D, Cornell CA. Incremental dynamic analysis. Earthq Eng Struct Dyn 2002;31:491–514. doi:10.1002/eqe.141.

[11] Elnashai AS, Kwon O-S. Fundamentals of Earthquake Engineering: From Source to Fragility. vol. 1.

2nd ed. 2015, John Wiley & Sons, Ltd.; 2015.

[12] Wang Z, Dueñas-Osorio L, Padgett JE. Optimal Intensity Measures for Probabilistic Seismic Response Analysis of Bridges on Liquefiable and Non-Liquefiable Soils. Struct. Congr. 2012, Reston, VA: American Society of Civil Engineers; 2012, p. 527–38. doi:10.1061/9780784412367.047.

[13] Wang X, Shafieezadeh A, Ye A. Optimal intensity measures for probabilistic seismic demand modeling of extended pile-shaft-supported bridges in liquefied and laterally spreading ground. Bull Earthq Eng 2018;16:229–57. doi:10.1007/s10518-017-0199-2.

[14] Mehanny SSF. A broad-range power-law form scalar-based seismic intensity measure. Eng Struct 2009;31:1354–68. doi:10.1016/j.engstruct.2009.02.003.

[15] Wang Z, Padgett JE, Dueñas-Osorio L. Influence of Vertical Ground Motions on the Seismic Fragility Modeling of a Bridge-Soil-Foundation System. Earthq Spectra 2013;29:937–62. doi:10.1193/1.4000170.

[16] Mohammed H. A Probabilistic Framework for Assessing Seismic Performance of Concrete Bridges Subjected to Spatial Variable Seismic Ground Motions. CAIRO UNIVERSITY, 2013.

[17] ECP-201. Egyptian Code of Practice no. 201 for determination of loads and forces for the structural and civil works. Cairo, Egypt: Research Centre for Housing and Construction, Ministry of Housing, Utilities and Urban Planning; 2012.

[18] ECP-203. Egyptian Code of Practice (2007), Design and Construction for Reinforced Concrete Structures. Cairo, Egypt: Ministry of Building Construction, Research Center for Housing, Building and Physical Planning; 2007.

[19] Kotb AA-M. Seismic Fragility of Continuous Bridges Considering Wave Passage and Soil-Structure Interaction Effects. Cairo University, 2019.

[20] Kotb AA-M, Mehanny SSF, Ramadan OOM. Effects of soil-structure interaction on the inelastic seismic response of continuous bridges on piled foundation. Int J Eng Adv Technol 2019;8. doi:10.35940/ijeat.F8503.088619.

[21] McKenna F. OpenSees: A Framework for Earthquake Engineering Simulation. Comput Sci Eng 2011;13:58–66. doi:10.1109/MCSE.2011.66.

[22] FIB-39. Fib Bulletin 39: Seismic bridge design and retrofit – structural solutions: state-of-art. Lausanne, Switzerland: The International Federation for Structural Concrete (fib); 2007.

[23] Ibarra LF, Medina RA, Krawinkler H. Hysteretic models that incorporate strength and stiffness deterioration. Earthq Eng Struct Dyn 2005;34:1489–511. doi:10.1002/eqe.495.

[24] Haselton CB, Deierlein GG. PEER Report 2007/08 Assessing Seismic Collapse Safety of Modern Reinforced Concrete Moment-Frame Buildings. Berkeley: 2008.

[25] Boulanger RW, Curras CJ, Kutter BL, Wilson DW, Abghari A. Seismic Soil-Pile-Structure Interaction Experiments and Analyses. J Geotech Geoenvironmental Eng 1999;125:750–9. doi:10.1061/(ASCE)1090-0241(1999)125:9(750).

[26] Boulanger RW, Kutter BL, Brandenberg SJ, Singh P, Chang D. Pile foundations in Liquefied and Laterally Spreading Ground during Earthquakes: Centrifuge Experiments & Analyses. California: 2003.

[27] Aygün B, Dueñas-Osorio L, Padgett JE, DesRoches R. Efficient Longitudinal Seismic Fragility Assessment of a Multispan Continuous Steel Bridge on Liquefiable Soils. J Bridg Eng 2011;16:93–107. doi:10.1061/(ASCE)BE.1943-5592.0000131.

[28] Barbosa AR, Mason HB, Romney KR. SSI-BRIDGE : SOIL-BRIDGE INTERACTION DURING

LONG-DURATION EARTHQUAKE MOTIONS. Corvallis: 2014.

[29] Wang Z, Dueñas-Osorio L, Padgett JE. Influence of Soil-Structure Interaction and Liquefaction on the Isolation Efficiency of a Typical Multispan Continuous Steel Girder Bridge. J Bridg Eng 2014;19:A4014001. doi:10.1061/(ASCE)BE.1943-5592.0000526.

[30] Yang Z, Lu J, Elgamal A. OpenSees Soil Models and Solid-Fluid Fully Coupled Elements User's Manual. California: 2008.

[31] Homaei F, Shakib H, Soltani M. Probabilistic Seismic Performance Evaluation of Vertically Irregular Steel Building Considering Soil–Structure Interaction. Int J Civ Eng 2017;15:611–25. doi:10.1007/s40999-017-0165-z.

[32] SEAOC. SEAOC Seismic design manual. Structural engineering association of California; 2000.

